Journal of Pharmaceutical & Biomedical Analysis
Vol. 8, No. 2, pp. 205–215, 1990
Printed in Great Britain

0731–7085/90 $3.00 + 0.00

On-line mass spectrometric investigation of the peroxidase-catalysed oxidation of uric acid*

KEVIN J. VOLK,† RICHARD A. YOST ‡ and ANNA BRAJTER-TOTH‡

Department of Chemistry, University of Florida, Gainesville, FL 32611, USA

Abstract: The enzymatic and electrochemical oxidation pathways of uric acid were determined on-line with thermospray–tandem mass spectrometry. Products and intermediates formed as a result of electrooxidation were monitored as the electrode potential was varied. Electrochemical results served as a model for the enzymatic studies. In fact, electrochemical studies were essential for elucidating the structures of intermediates because of the high conversion efficiencies in electrooxidation. Products and intermediates formed as a result of enzymatic oxidation of uric acid were monitored as the reaction time was varied. When the enzymatic oxidation of uric acid with peroxidase and H_2O_2 was studied, the same intermediates and products were observed as in the electrochemical oxidation. The tandem mass spectrometric results provide convincing evidence that the primary intermediate produced during both the enzymatic and electrochemical oxidation of uric acid has a quinonoid diimine structure. The primary intermediate can follow three distinct reaction pathways to produce the identified final products. The final enzymatic and electrochemical oxidation products observed in these studies were urea, CO_2, alloxan, alloxan monohydrate, allantoin, 5-hydroxyhydantoin-5-carboxamide and parabanic acid.

Keywords: *Enzyme reactor; electrooxidation; thermospray; tandem mass spectrometry; reversed-phase liquid chromatography.*

Introduction

Modern electrochemical methods have recently been used to investigate the redox chemistry of many biologically significant molecules as well as many important synthetic compounds [1–12]. The premise of these studies has been that electrochemical methods can provide useful and unique insights into the pathways and mechanisms of enzymatic redox reactions of such molecules. There are many excellent examples of the unique insights into biological–redox reactions provided by electrochemistry [1–12]. Work of Dryhurst *et al.* has shown considerable similarity between the pathways of the electrochemical and peroxidase-catalysed oxidation of uric acid [11]. In these studies electrochemical measurements were successfully combined with spectroelectrochemistry, gel-permeation chromatography, liquid chromatography and off-line gas chromatography–mass spectrometry (GC–MS) to provide a complete picture of the reaction products. However, these techniques could provide only limited information about intermediates [12] and the dynamic solution reactions which followed the initial electrochemical and enzymatic oxidation.

In recent reports from this laboratory [13, 14], it has been shown that coupling electrochemistry on-line with thermospray–tandem mass spectrometry (EC–TSP–MS–MS; Fig. 1) can provide detailed redox information about biologically significant molecules. The method allows simple detection of intermediates and products formed in the electrooxidation. Because thermospray provides mainly molecular-weight information, structural assignments of intermediates and products requires tandem mass spectrometry [13, 14]. In addition, the use of MS–MS allows identification of intermediates and products in the reaction mixture based on their characteristic daughter spectra without a need for further separation, a feature important to the identification of structurally related metabolites [15, 16].

The main objective of this work was to determine the capabilities of TSP–MS–MS to monitor dynamic on-line enzymatic reactions. For this purpose, the enzymatic reaction of uric acid was investigated on-line with TSP–MS–MS. This paper demonstrates that a complete interpretation of the peroxidase-catalysed oxidation of uric acid is possible with an enzyme reactor coupled on-line with a thermospray–tandem mass spectrometer. The electro-

*Presented at a Symposium at the 40th Pittsburgh Conference and Exposition, Atlanta, Georgia, March 1989.
†Current address: Ciba-Geigy Corp., Ardsley, NY 10502, USA.
‡Authors to whom correspondence should be addressed.

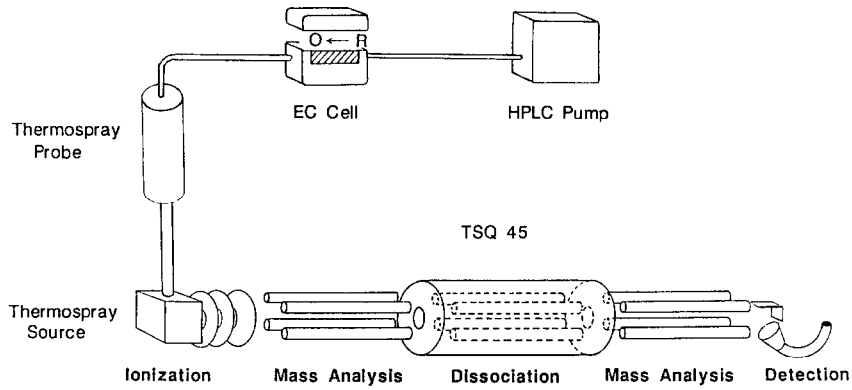

Figure 1
On-line EC–TSP–MS–MS system.

chemical results served as a model for the interpretation of the on-line enzymatic data.

Experimental

Apparatus

A Finnigan MAT TSQ 45 tandem quadrupole mass spectrometer equipped with a Vestec thermospray LC–MS interface and INCOS data system was used for all studies. The mobile phase was delivered with a Rainin MacRabbit HPLC gradient system at a flow rate of 2.0 ml min^{-1}. In the electrochemical studies, samples were injected with a Rheodyne (model 7410) injector fitted with a 20-μl loop. Typically, 20 μl of a 90 ppm solution of uric acid were injected. The ESA electrochemical cell (Bedford, MA) has been described previously [13].

LC procedure

The intermediates and products of the electrochemical oxidation of uric acid were separated by high-performance liquid chromatography (LC) using a Microsorb (Rainin) C_{18} reversed-phase column (15 cm × 4.6 mm, i.d.) with mass spectrometric detection. All experiments were performed with a Rainin MacRabbit HPLC gradient system. The separation was isocratic with aqueous 0.1 M ammonium acetate–methanol (pH*5.0; 98:2, v/v) as a mobile phase at a flow rate of 2.0 ml min^{-1}. With a small percentage of methanol in the mobile phase, operating the thermospray interface in the filament-on mode was important for the thermospray ionization of uric acid. Methanol was added to facilitate detection of the $[M—H]^-$ ion of uric acid, which was otherwise difficult to observe. Optimum operating temperatures were not affected by the presence of such small quantities of methanol. Intermediates and products formed as a result of methanolysis reactions were only detected when higher percentages of methanol (>15%, v/v) were used.

Reagents

Uric acid, hydrogen peroxide, and type VIII horseradish peroxidase (EC 1.11.1.7) were obtained from Sigma (St. Louis, MO). The reagents were used as received. In all enzymatic studies, uric acid was dissolved in, and then injected into, a mobile phase which consisted of aqueous 0.1 M ammonium acetate (pH ~5.0) containing 50 μM hydrogen peroxide. Twenty microliters of a 50 μg ml^{-1} solution were injected.

Enzyme binding procedure

In order to prepare an enzyme reactor, 40 mg of type VIII horseradish peroxidase were dissolved in 50 ml of 0.1 M phosphate buffer (pH ~7) and were recirculated through a Hydropore-EP Affinity (Rainin) column (10 cm × 4.6 mm, i.d.) for 24 h at a flow rate of 0.1 ml min^{-1}. The Hydropore-EP Affinity stationary phase consisted of a modified hydrocarbon-spacer arm attached to a silica support. The enzyme, which contains primary amine functional groups, reacts with the epoxide moiety located on the end of the spacer arm and forms a covalent bond with the stationary phase. Upon completion of the binding procedure, the column was flushed with 50 ml of 0.1 M phosphate buffer (pH ~7) and stored in phosphate buffer at 10°C. The enzyme solu-

tion, ammonium acetate buffer, and phosphate buffer solutions were filtered through a 0.45-μm filter before use.

Mass spectrometry

The thermospray interface (Vestec Corp., Houston, TX) was mounted on a triple stage quadrupole mass spectrometer (Finnigan Corp., San Jose, CA, Model TSQ 45). The thermospray interface was operated in the filament-on mode, in contrast with our previous studies [13, 14], which did not employ a filament. The filament-on mode was used to improve sensitivity for uric acid. Two temperatures were monitored in the experiments: the vaporizer exit temperature (tip temperature) and the source block temperature. At a flow rate of 2.0 ml min^{-1}, the typical operating temperatures were tip, 238°C, and source, 290°C.

Both positive ion and negative ion thermospray mass spectra were obtained by pulsed positive ion–negative ion chemical ionization (PPINICI) [13]. Typical conditions for TSP–MS were scan range from mass-to-charge ratio (m/z) 120 to 300 in 0.3 s, electron multiplier voltage 1000 V, and preamplifier gain 10^8 VA^{-1}. For MS–MS, the scan range and rates varied depending upon the m/z of the parent ion. Collisionally activated dissociation (CAD) studies were carried out using nitrogen as the collision gas (2 mtorr) with a collision energy of 30 eV.

Results and Discussion

Characterization of the oxidation pathway by on-line EC–TSP–MS–MS

The oxidation pathway of uric acid was first characterized by EC–TSP–MS–MS to serve as a model for the enzymatic work. At pH 7.0 uric acid is known [1, 4, 11, 12] to undergo a $2e^-$, $2H^+$ electrochemical oxidation at *ca* +0.40 V versus SCE to form an unstable intermediate with a proposed quinonoid diimine structure (Fig. 2). This intermediate is highly susceptible to nucleophilic attack by water, ammonia and methanol. This was verified and the structures of the secondary intermediates resulting from these nucleophilic reactions were identified and characterized by EC–TSP–MS–MS [13–14]. The negative ion daughter mass spectral data of these secondary intermediates are tabulated in Table 1. Each of the identified ions listed in Table 1 produces a unique fragmentation pattern, which provides the necessary information to elucidate its structure. Losses of small neutral molecules such as NH_3, CONH, HCN, CO or H_2O were common during the CAD of even-electron species such as $[M - H]^-$ ions, as can be seen in Table 1.

Figure 3 shows the electrochemical oxidation pathway of uric acid which is based upon EC–TSP–MS–MS results [13, 14]. As can be seen in Fig. 3 and Table 1, the intermediates resulting from partial hydrolysis (M_W 184) and

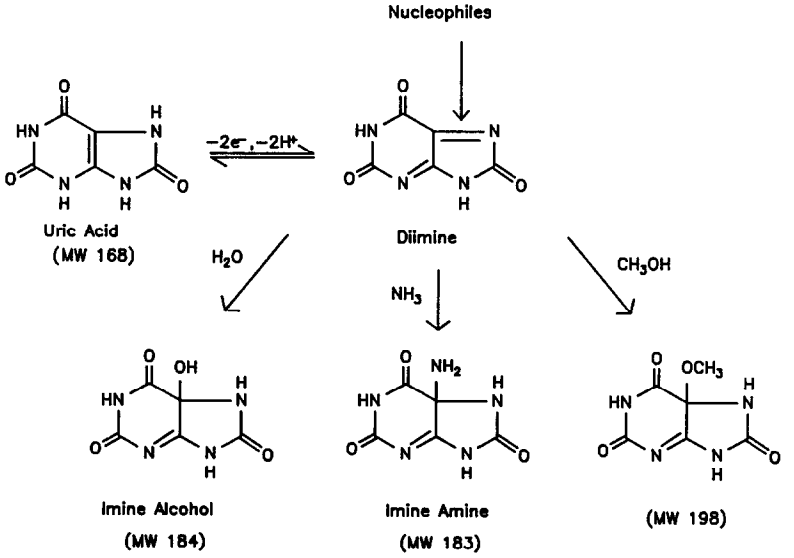

Figure 2
Electrooxidation of uric acid, followed by nucleophilic addition of water, ammonia and methanol to the primary diimine intermediate to form secondary intermediates.

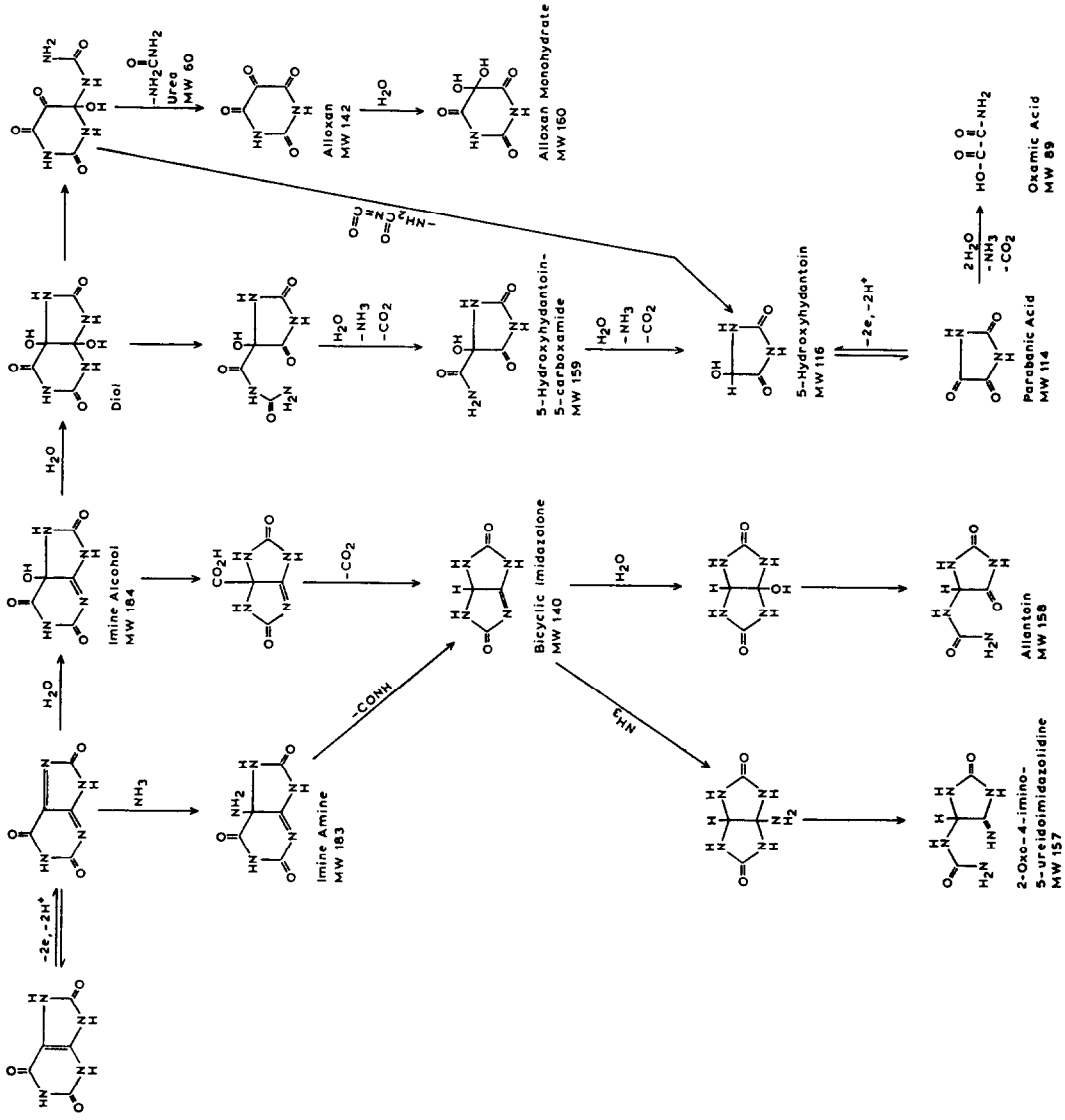

Figure 3
Oxidation pathway of uric acid. The molecular weights are shown for those intermediates and products which have been identified by EC–TSP–MS and EC–TSP–MS–MS.

Table 1
Negative ion daughter mass spectra of identified oxidation intermediates of uric acid

m/z	(% RA)*	Structure correlation
$[M - H]^-$ ion of the imine amine at *m/z* 182		
182	(22)	Parent ion
139	(100)	Loss of CONH from 182^-
112	(7)	Loss of HCN from 139^-
96	(53)	Loss of CONH from 139^-
69	(11)	Loss of HCN from 96^-
42	(23)	Loss of HCN from 69^-
$[M - H]^-$ ion of the imine alcohol at *m/z* 183		
183	(25)	Parent ion
140	(100)	Loss of CONH from 183^-
112	(8)	Loss of CO from 140^-
97	(90)	Loss of CONH from 140^-
69	(3)	Loss of CO from 97^-
42	(8)	Loss of HCN from 69^-
$[M - H]^-$ ion of methanolysis intermediate at *m/z* 197		
197	(50)	Parent ion
196	(20)	Loss of H· from 197^-
182	(10)	Loss of CH_3· from 197^-
165	(8)	Loss of CH_3OH from 197^-
154	(100)	Loss of CONH from 197^-
153	(10)	Loss of CONH from $196^{-\cdot}$
139	(15)	Loss of CH_3· from 154^-
127	(15)	Loss of HCN from 154^-
126	(15)	Loss of CO from 154^-
122	(10)	Loss of CH_3OH from 154^-
111	(10)	Loss of CONH from 154^-
97	(8)	Loss of CON· from $139^{-\cdot}$

*Percent relative abundance.

partial ammonolysis (M_W 183) of the quinonoid diimine have been positively identified by their respective fragmentation patterns in EC–TSP–MS–MS. The final electrochemical oxidation products (urea, CO_2, alloxan, alloxan monohydrate, allantoin, 5-hydroxyhydantoin-5-carboxamide and parabanic acid) must have resulted from the imine-alcohol and the imine-amine intermediates undergoing additional nucleophilic reactions and rearrangements (Fig. 3). Although these reactions occur in solution at ambient temperatures [11, 12], the short residence time in the system at ambient temperatures and subsequent contact with the hot thermospray vaporizer probe caused them to occur primarily in the probe. Some of these products have been identified in previous off-line studies [1, 12] using classical GC–MS techniques. However, on-line tandem mass spectrometry provides an additional separation stage which allows the mixture of intermediates and products to be identified by their respective fragmentation patterns without chromatographic separation [13, 14]. The methanolysis intermediate and products which also form [14] are not shown in Fig. 3.

Mass spectrometric hydrodynamic voltammograms of uric acid

One of the important advantages of coupling electrochemistry on-line with MS is the ability to monitor dynamic reactions which occur in aqueous solution. Figure 4 illustrates the mass spectrometric hydrodynamic voltammograms of uric acid obtained by EC–TSP–MS. As shown by the cyclic voltammogram obtained under normal conditions in stationary solution at a small electrode (about 0.05 cm^2), oxidation of uric acid begins to occur at about +0.0 V versus a Pd reference and proceeds at a maximum rate at about +0.40 V. Electrochemical oxidation of uric acid in a flowing stream through a porous electrode, as monitored on-line by MS, is shown in Fig. 4. The oxidation process can be followed by monitoring the intensity of the $[M - H]^-$ ion of uric acid at *m/z* 167 as a function of the electrode potential. The intensity of the *m/z* 167 ion, in agreement with the response shown by cyclic voltammetry, decreases due to the oxidation of uric acid as the electrode potential becomes more positive than +0.0 V versus Pd. Intensities of the ions corresponding to the intermediates (e.g. imine alcohol, $[M - H]^-$ *m/z* 183, Fig. 4) and the products (e.g. allantoin, $[M - H]^-$ *m/z* 157, Fig. 4) of uric acid oxidation, which can also be monitored by MS,

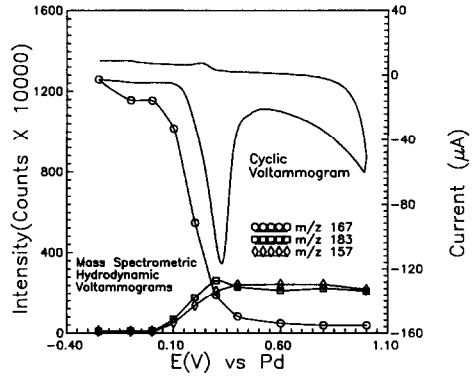

Figure 4
Mass spectrometric hydrodynamic voltammograms of uric acid; *m/z* 167 = $[M - H]^-$ of uric acid, *m/z* 183 = $[M - H]^-$ of imine alcohol, *m/z* 157 = $[M - H]^-$ of allantoin. Flow rate of 0.1 M ammonium acetate mobile phase 2.0 ml min^{-1}. Tip temperature 240°C and source temperature 290°C. Cyclic voltammogram of 300 μM uric acid on rough pyrolytic graphite. Scan rate of 200 mV s^{-1}. Palladium reference electrode and 0.1 M ammonium acetate supporting electrolyte.

increase with increasing electrode potential. A steady-state response is observed for all ions at potentials >+0.40 V where the oxidation rate reaches a maximum due to the hydrodynamic flow of reactant [17], in agreement with the cyclic voltammetric results (Fig. 4).

Insights into the reaction pathway provided by EC–LC–TSP–MS

It was postulated that many of the hydrolysis and rearrangement reactions of the imine alcohol occurred in the hot vaporizer probe. The half-life of the imine-alcohol intermediate (M_W 184) in solution at 25°C has been estimated by spectroelectrochemistry as about 2 min [11]. As a result, detection of the final products by EC–TSP–MS was not anticipated because at a flow rate of 2.0 ml min^{-1} the time from the initiation of the electrooxidation in the electrochemical cell to detection by MS is about 500 ms [14]. However, since all of the final products were observed, LC was used on-line with the electrochemical cell to separate electrochemically generated products prior to analysis by EC–LC–TSP–MS–MS in order to verify their place of origin. If the products in Fig. 3 were formed in solution immediately after electrooxidation at about 0.40 V, then more than one chromatographic peak would be expected after their separation. If, on the other hand, the products were formed later in the thermospray vaporizer probe, one LC peak would be expected since it was the electrochemically generated imine alcohol intermediate which would be expected to elute through the LC column and eventually lead to product formation.

Figure 5 illustrates the LC–TSP negative ion $[M - H]^-$ mass chromatograms of a two-component standard mixture of allantoin (M_W 158) and uric acid (M_W 168), which are chromatographically separated in <2 min. As can be seen in Fig. 5, allantoin eluted immediately after the solvent peak, indicated in Fig. 5 by an arrow. The on-line EC–LC–TSP–MS results obtained for the electrochemical oxidation of uric acid can be seen in Fig. 6. The negative ion mass chromatograms indicated only one peak eluting during the HPLC separation. As can be seen in Fig. 6, the compound(s) eluting at this peak were not retained and the retention time of authentic allantoin was different (Fig. 5). The fact that the imine-alcohol intermediate, bicyclic-imidazolone intermediate, and the final products, allantoin and alloxan, all originated from the same peak

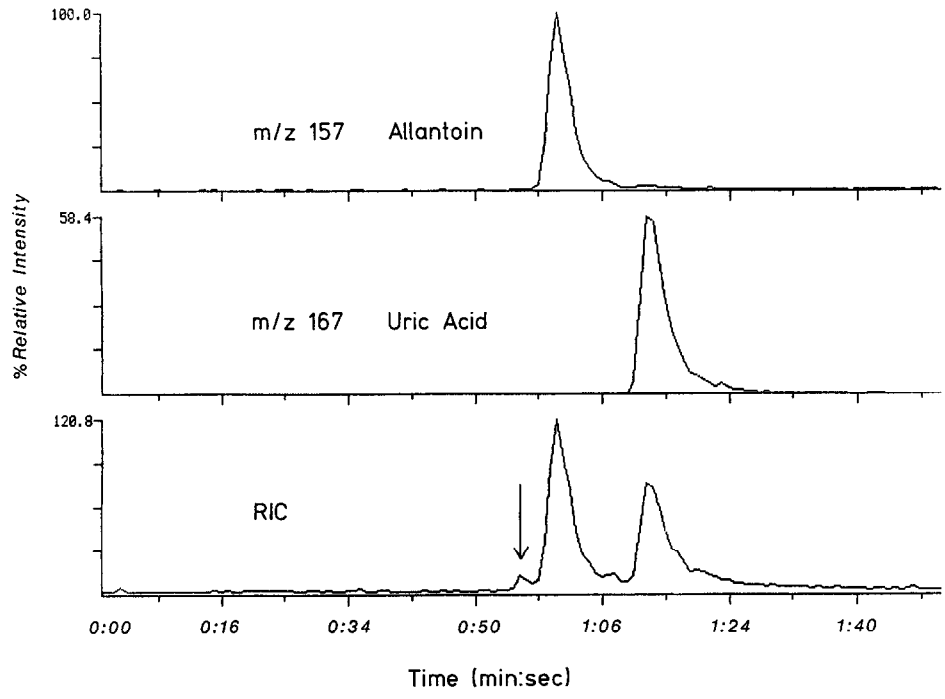

Figure 5
LC–TSP–MS negative ion mass chromatograms of a mixture containing allantoin and uric acid. The solvent peak in the reconstructed ion chromatogram (RIC) is indicated by an arrow. Mobile phase 0.1 M ammonium acetate–methanol (pH 5.0 98:2, v/v) at a flow rate of 2.0 ml min^{-1}. Tip temperature 238°C, source temperature 300°C.

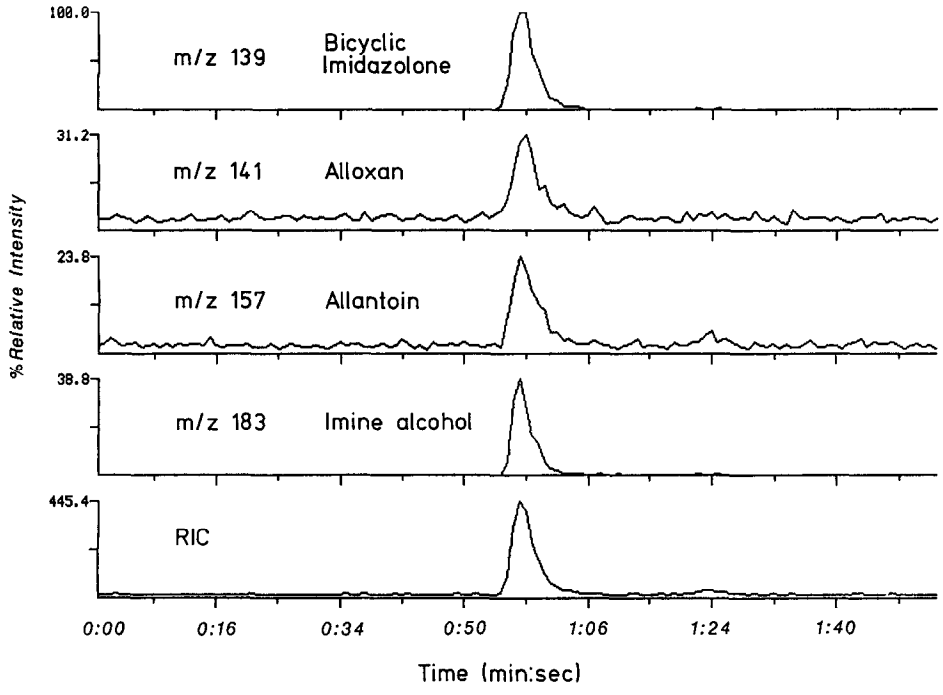

Figure 6
EC–LC–TSP–MS negative ion mass chromatograms of the oxidation products of uric acid at +0.50 V. Mobile phase 0.1 M ammonium acetate–methanol (pH* 5.0 0.98:2, v/v) at a flow rate of 2.0 ml min^{-1}. Tip temperature 238°C, source temperature 300°C.

eluting at the solvent front (about 1 min) indicated that the reactions which lead to their formation occurred after LC separation, and therefore somewhere during the thermospray ionization process. Although not shown in Fig. 6, the negative ion mass chromatogram of the $[M - H]^-$ ion of uric acid at *m/z* 167 did not show any signal above the normal background, indicating that uric acid had been completely oxidized or was present at concentrations below the detection limit of the TSP–MS system. The conversion efficiency of this system has been estimated at about 85% [14].

The unique operating conditions of EC–TSP–MS–MS made it possible to detect intermediates as well as final products after electrooxidation. The rapid temperature changes which occurred during the thermospray vaporization process altered the kinetics of the reactions responsible for product formation. Because the temperatures changed from 25 to 240°C in <500 ms during the thermospray process, the rate constants for the disappearance of the intermediates could not be compared readily with the values obtained by spectroelectrochemistry at room temperature [11, 12]. However, despite a delay time of only 500 ms, the elevated temperatures in EC–TSP–MS make it possible to observe the final products.

Comparison of electrochemical and enzymatic oxidation of uric acid

Previous off-line studies on the enzymatic oxidation of uric acid have shown that type VIII horseradish peroxidase exhibits high activity towards uric acid at pH ~5.0 [18]. For the on-line enzyme–TSP–MS studies, an enzyme reactor with the covalently-bonded horseradish peroxidase was produced (Experimental). The primary goal of these studies was to assess the capability of TSP–MS to monitor the enzymatic reaction on-line. Because of the similarities observed in the previous off-line studies of the electrochemical and peroxidase-catalysed oxidation of uric acid [11, 12, 18], it was anticipated that on-line EC–TSP–MS–MS [13, 14] would serve as a useful model in the present work.

The amount of time that the substrate, uric acid, reacted with the enzyme could be varied by changing the flow rate of the mobile phase through the enzyme reactor. Since thermospray is a flow-rate dependent technique, a tee-piece was placed after the enzyme column and make-up flow from another pump was used so

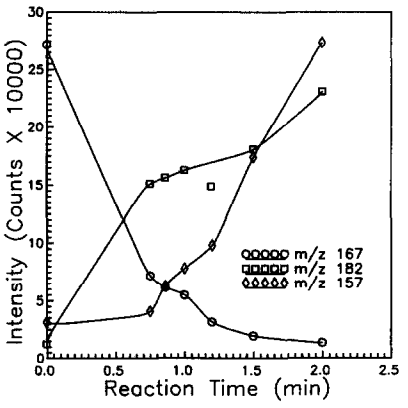

Figure 7
Mass spectrometric monitoring of intermediates and products produced during the perioxidase-catalysed oxidation of uric acid; *m/z* 167 = $[M - H]^-$ of uric acid, *m/z* 183 = $[M - H]^-$ of imine alcohol, *m/z* 157 = $[M - H]^-$ of allantoin. Mobile phase ammonium acetate (pH 5.0, 0.1 M) (50 μM H_2O_2) at a total flow rate of 2.0 ml min^{-1}. Tip temperature 238°C, source temperature 300°C.

that the thermospray interface always operated at a combined flow rate of 2.0 ml min^{-1}. Figure 7 illustrates the intensities of the $[M - H]^-$ ions of uric acid (M_W 168), imine amine intermediate (M_W 183), and the final product allantoin (M_W 158) as a function of enzymatic reaction time. The data at zero time were obtained without the enzyme reactor. The intensity of the $[M - H]^-$ ion of uric acid at *m/z* 167 decreased as the enzymatic reaction time increased as a result of increasingly complete enzymatic conversion. Consequently, as the reaction time increased the intensities of the ions corresponding to intermediates (e.g. imine amine, $[M - H]^-$ *m/z* 182, Fig. 3) and product (e.g. allantoin, $[M - H]^-$ *m/z* 157, Fig. 3) of uric acid oxidation increase. Because it was considered possible for uric acid to undergo non-enzymatic oxidation in the presence of H_2O_2, the H_2O_2 oxidation of a structurally similar compound, 9-methyl uric acid, was also examined. The methyl derivative was chosen because it produces a more intense thermospray signal. The enzymatic and electrochemical properties of 9-methyl uric acid are very similar to those of uric acid [11, 19, 20]. The addition of 50 μM H_2O_2 to a solution of 50 μg ml^{-1} 9-methyl uric acid did not cause any detectable oxidation during a 30-min time period at room temperature, or during the thermospray process.

To characterize the intermediates and products formed in the enzymatic oxidation, both the positive ion and negative ion thermospray mass spectra were examined [13]. This was because certain species had favourable proton affinities to produce only an $[M + H]^+$ ion or an $[M - H]^-$ ion via gas-phase proton transfer reactions with the ammonium acetate buffer [13]. However, some compounds can undergo both reactions. The latter case was ideal for identifying the molecular weights of unknown intermediates and products [13]. Figures 8a and 8b illustrate typical electrochemistry–thermospray positive ion and negative ion mass spectra of the oxidation intermediates and products of uric acid. Table 2 summarizes the molecular, adduct and fragment ions identified when the lower scan limit of the mass spectrometer was reduced from *m/z* 120 to *m/z* 30. Those ions in Figs 8a and 8b which have been identified have been marked with an asterisk. Figure 3 shows the oxidation pathway of uric acid which is based on the EC–TSP–MS–MS results.

The positive and negative ion mass spectra of the enzymatic oxidation intermediates and products obtained when the uric acid substrate

Table 2
Positive and negative ions identified in the EC–TSP–MS–MS of uric acid

m/z	Identity
Positive ions	
45	$[CO_2+H]^+$
61	$[Urea+H]^+$
120	$[Urea+Acetamide+H]^+$
121	$[Urea+Urea+H]^+$
134	$[5\text{-Hydroxyhydantoin}+NH_4]^+$
141	$[Bicyclic\ imidazolone+H]^+$
143	$[Alloxan+H]^+$
158*	$[2\text{-Oxo-4-imino-5-ureidoimidazolidine}+H]^+$
159	$[Allantoin+H]^+$
176	$[Allantoin+NH_4]^+$
177	$[5\text{-Hydroxyhydantoin-5-carboxamide}+NH_4]^+$
184*	$[Imine\ amine+H]^+$
200	$[Bicyclic\ imidazolone+acetamide+H]^+$
201*	$[imine\ amine+NH_4]^+$
Negative ions	
88	$[Oxamic\ acid-H]^-$
113	$[Parabanic\ acid-H]^-$
115	$[Alloxan\ monohydrate-CO_2-H]^-$
139	$[Bicyclic\ imidazolone-H]^-$
141	$[Alloxan-H]^-$
156*	$[2\text{-Oxo-4-imino-5-ureidoimidazolidine}-H]^-$
157	$[Allantoin-H]^-$
158	$[5\text{-Hydroxyhydantoin-5-carboxamide}-H]^-$
167	$[Uric\ acid-H]^-$
175	$[Alloxan\ monohydrate-CO_2+acetate]^-$
182*	$[Imine\ amine-H]^-$
183	$[Imine\ alcohol-H]^-$
201	$[Alloxan+acetate]^-$

* Produced in ammonolysis reactions at tip temperatures <240°C.

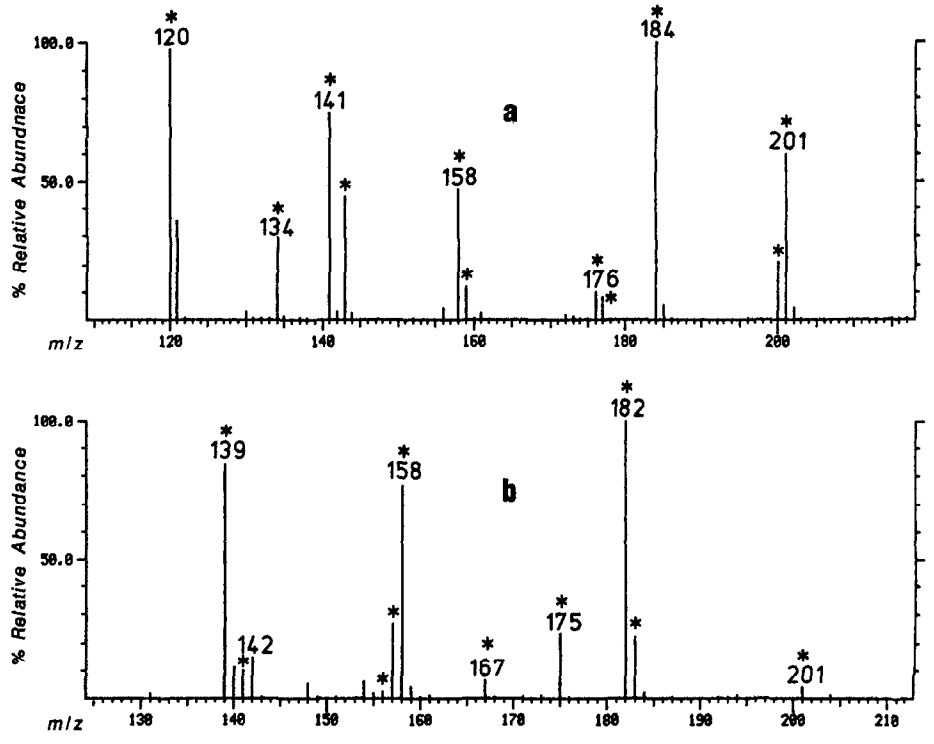

Figure 8
Positive ion (a) and negative ion (b) spectra of the electrochemical oxidation intermediates and products of uric acid. Tip temperature 238°C and source temperature 290°C.

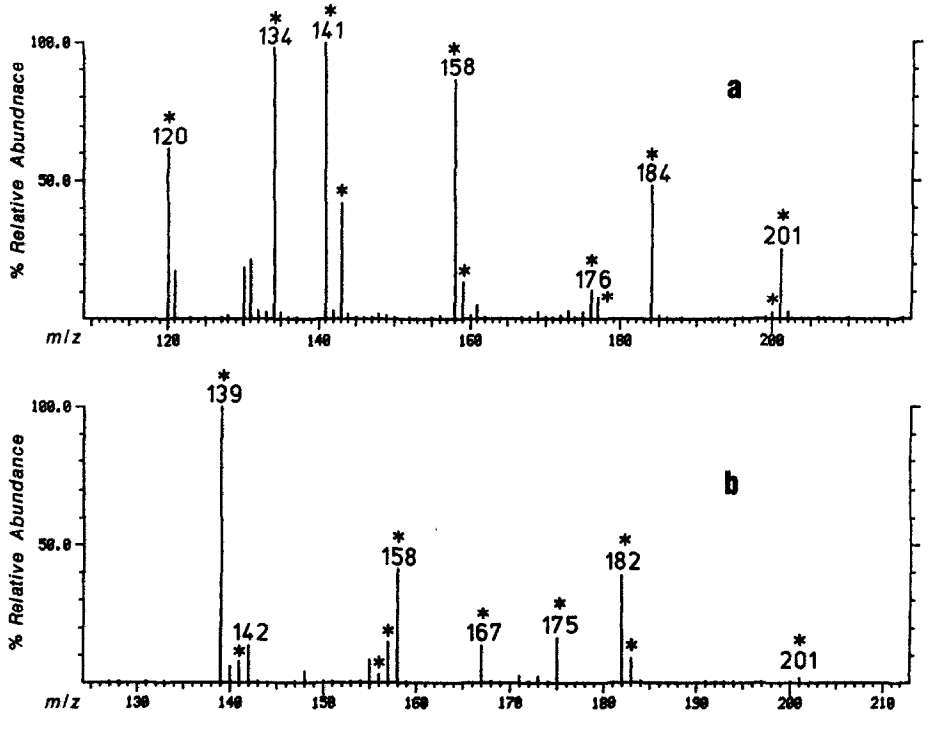

Figure 9
Positive ion (a) and negative ion (b) spectra of the enzymatic oxidation intermediates and products of uric acid. Enzyme–substrate reaction time of 1 min. Tip temperature 238°C and source temperature 290°C.

residence time in the reactor was approximately 1 min are shown in Figs 9a and 9b. Comparison of the mass specta obtained from the peroxidase-catalysed and the electrochemical oxidation of uric acid showed that the intermediates and products formed in the enzymatic oxidation were the same as those formed in the electrochemical oxidation. However, the positive ion mass spectrum of the enzymatic oxidation products contained two as yet unidentified ions (130^+, 131^+) which were not present in the electrochemical mass spectrum.

Although most of the same ions are present in both the electrochemical and enzymatic mass spectra, their relative abundances were different. The product–intermediate intensity ratios $134^+/184^+$ ([5-hydroxyhydantoin + NH_4]$^+$/[imine amine + H]$^+$) and $175^-/182^-$ ([alloxan monohydrate − CO_2 + acetate]$^-$/[imine amine − H]$^-$) were an indication of the degree of completeness of the reactions which follow the initial oxidation process (Fig. 3, Table 2). For example, the electrochemical oxidation was characterized by a $134^+/184^+$ intensity ratio of 0.30 and a $175^-/182^-$ intensity ratio of 0.25 (Figs 8a and 8b). However, in the enzymatic oxidation the $134^+/184^+$ intensity ratio was 1.8, whereas the $175^-/182^-$ intensity ratio was 0.45 (Figs 9a and 9b). These intensity ratios indicated that the hydrolysis reactions of the oxidation intermediates (Fig. 3) had proceeded to a greater extent in the enzymatic oxidation. The enzymatically generated intermediates had a much longer residence time in solution (1 min) than the electrochemical intermediates (500 ms) and this accounts for the different intensity ratios. For example, during the 1 min enzymatic reaction period, some of the imine-alcohol and imine-amine (Fig. 3) could have decayed to the bicyclic imidazolone as well as to the final products. This was apparent from the greater relative abundances of the 139^- and the 141^+ ions in Figs 9a and 9b which correspond to the $[M - H]^-$ and $[M + H]^+$ of the bicyclic imidazolone.

It is clear from these studies that EC–TSP–MS–MS serves as a useful model for the on-line enzyme–TSP–MS work. Unfortunately, the peaks detected following enzymatic oxidation were much broader (peak width ~14 s) because of dispersion after a 1-min reaction than were the peaks following electrochemical oxidation (peak width ~4 s). In addition, the make-up flow added at the tee diluted the reaction mixture as it exited the enzyme reactor. These two factors contributed to the low intensities observed for the enzymatic studies (compare the intensity scales in Figs 4 and 7) and prevent acquisition of reasonable daughter mass spectra by MS–MS. As can be seen in Fig. 7, the uric acid $[M - H]^-$ ion decreased to ~15% of its original intensity after a 1-min reaction, indicating high enzymatic conversion efficiencies (about 85%), comparable to those obtained electrochemically.

Since the electrochemical and enzymatic thermospray mass spectra (Figs 8a, 8b, 9a and 9b) were virtually identical, both reactions must have followed similar reaction pathways. Therefore, it is reasonable to postulate that the structures of the intermediates and products elucidated by EC–TSP–MS–MS reflected those of the enzymatically generated compounds of the same *m/z* ratio. This is supported by a close match between the mass spectral data obtained in the enzymatic and electrochemical oxidation of uric acid. Hence, the observation of the imine-alcohol and the imine-amine intermediates during the peroxidase-catalysed oxidation supports the formation of a quinonoid diimine intermediate (Fig. 2) after the enzymatic oxidation of uric acid.

Enzyme columns have been previously combined on-line with TSP–MS for protein sequencing [21, 22]. However, this work clearly shows that enzymatic reactors coupled on-line with TSP–MS can provide useful information about both intermediates and products formed during an enzymatic reaction. The methods described in this paper can be used to obtain useful information about the pathways of other biological redox reactions; this work is being pursued.

Acknowledgements — This research was supported in part by grants from the US Chemical Research Development and Engineering Center (RAY, ABT), the National Institutes of Health (ABT), the Division of Sponsored Research at the University of Florida (RAY, ABT), and the Interdisciplinary Center for Biotechnology Research at the University of Florida (ABT). KJV thanks Merck-Dohme for a graduate fellowship.

References

[1] G. Dryhurst, in *Electrochemistry of Biological Molecules*. Academic Press, New York (1977).
[2] K. McKenna and A. Brajter-Toth, *J. Electroanalyt. Chem.* **233**, 49–62 (1987).

[3] P.J. Kraske and A. Brajter-Toth, *J. Electroanalyt. Chem.* **207**, 101–116 (1986).
[4] R.N. Goyal, A. Brajter-Toth and G. Dryhurst, *J. Electroanalyt. Chem.* **131**, 181–202 (1982).
[5] T.E. Childers-Peterson and A. Brajter-Toth, *J. Electroanalyt. Chem.* **239**, 161–173 (1988).
[6] T.E. Childers-Peterson and A. Brajter-Toth, *Analytica Chim. Acta* **202**, 167–174 (1987).
[7] D. Astwood, T. Lippincott, M. Deysher, C. D'Amico, E. Szurley and A. Brajter-Toth, *J. Electroanalyt. Chem.* **159**, 295–312 (1983).
[8] D.J. Miner, J.R. Rice, R.M. Riggin and P.T. Kissinger, *Analyt. Chem.* **53**, 2258–2263 (1981).
[9] J.R. Rice and P.T. Kissinger, *Biochem. Biophys. Res.* **104**, 1312–1318 (1982).
[10] P.A. Andrews, Su-Shu Pan and N.R. Bachur, *J. Am. Chem. Soc.* **108**, 4158–4166 (1986).
[11] G. Dryhurst, K.M. Kadish, F. Scheller and R. Renneberg, in *Biological Electrochemistry*. Academic Press, New York (1982).
[12] A. Brajter-Toth and G. Dryhurst, *J. Electroanalyt. Chem.* **122**, 205–213 (1981).
[13] K.J. Volk, M.S. Lee, R.A. Yost and A. Brajter-Toth, *Analyt. Chem.* **60**, 720–722 (1988).
[14] K.J. Volk, R.A. Yost and A. Brajter-Toth, *Analyt. Chem.* **61**, 1709–1717 (1989).
[15] R.J. Perchalski, R.A. Yost and B.J. Wilder, *Analyt. Chem.* **54**, 1466–1471 (1982).
[16] P. Rudewicz and K.M. Straub, *Analyt. Chem.* **58**, 2928–2934 (1986).
[17] P.T. Kissinger and W.R. Heineman, in *Laboratory Techniques in Electroanalytical Chemistry*. Marcel Dekker, New York (1984).
[18] H.A. Marsh and G. Dryhurst, *J. Electroanalyt. Chem.* **95**, 81–90 (1979).
[19] M.Z. Wrona, J.L. Owens and G. Dryhurst, *J. Electroanalyt. Chem.* **105**, 295–315 (1979).
[20] M.Z. Wrona and G. Dryhurst, *Biochim. Biophys. Acta* **570**, 371–387 (1979).
[21] H.Y. Kim, D. Pilosof, D.F. Dyckes and M.L. Vestal, *J. Am. Chem. Soc.* **106**, 7304–7309 (1984).
[22] K. Stachowiak, C. Wilder, M.L. Vestal and D.F. Dyckes, *J. Am. Chem. Soc.* **110**, 1758–1765 (1988).

[Received for review 10 March 1989; revised version received 11 April 1989]